J. Fluid Mech. (1972), *vol.* 56, *part* 4, *pp.* 803–813
Printed in Great Britain

Note on the rheology of a dilute suspension of dipolar spheres with weak Brownian couples

By E. J. HINCH
Department of Applied Mathematics and Theoretical Physics, University of Cambridge
AND L. G. LEAL
Chemical Engineering, California Institute of Technology

(Received 24 July 1972)

A problem of theoretical interest in suspension rheology is the calculation of bulk rheological properties for a dilute suspension of spherical dipolar particles in the presence of weak Brownian rotation, when the applied field is perpendicular to the local vorticity of the bulk flow. In the present note, we determine the asymptotic form for the orientation distribution of the dipole axis in the limit of weak Brownian motion and use this distribution to determine the corresponding rheological properties of the suspension. The bulk stress is then discussed in terms of an effective viscosity for shear flow.

1. Introduction

In a recent paper, Brenner & Weissman (1972) have considered the effects of rotary Brownian motion on the rheology of a dilute suspension of rigid dipolar spheres in the presence of an applied external field. Using both numerical and analytical approximation schemes, these authors were able to consider a variety of combinations of field direction and strength, and effective strength of the rotary Brownian motion. Among the cases which were either partially or totally unresolved, the most interesting is that in which the applied field is perpendicular to the local vorticity of the bulk flow, and the field strength is moderately weak ($\gamma = \frac{1}{2}\pi$, $\lambda \leqslant 1$ in Brenner & Weissman's notation). In the present note, we investigate this case in the limit of weak Brownian motion.

2. The basic equations

We consider a dilute suspension of rigid, spherical dipolar particles which is undergoing a steady bulk flow in the presence of an applied external field $\mathbf{g}$. Since the suspension is dilute, attention can be focused upon the behaviour of a single isolated particle. We denote the magnitude of the particle's permanent dipole moment by m and its orientation by the unit vector $\mathbf{e}$. Neglecting inertia effects on the small scale of the suspended particles, the motion of an isolated particle in the absence of rotary Brownian motion is then determined by the

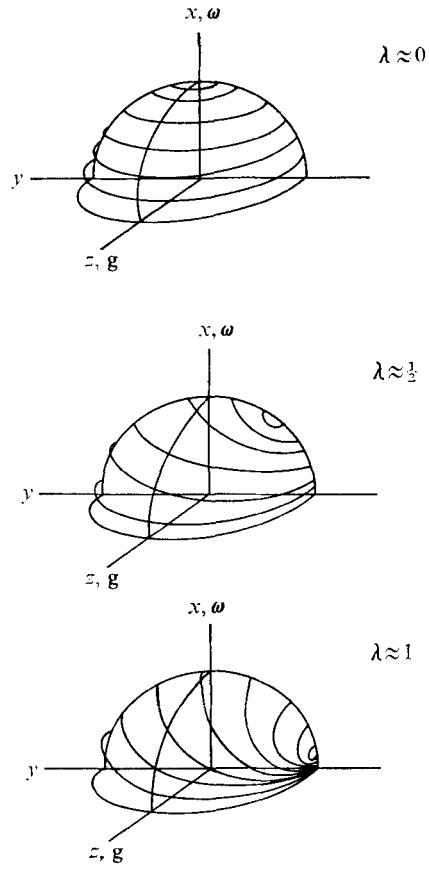

FIGURE 1. Typical orbit paths for $\lambda \cong 0, \frac{1}{2}, 1$.

condition that the hydrodynamic and external field couples exactly balance one another. This yields the rate of rotation of the dipole axis:

$$\dot{\mathbf{e}} = \boldsymbol{\omega} \times \mathbf{e} + \frac{m}{8\pi\mu a^3}[\mathbf{g} - \mathbf{e}(\mathbf{e}.\mathbf{g})], \tag{1}$$

in which $\boldsymbol{\omega}$ is the local vorticity of the bulk flow, a the radius of the sphere and μ the solvent viscosity. The dimensionless measure of the field strength is $\lambda = mg/8\pi\mu a^3\omega$. The solution of (1) depends on λ and on the angle γ between $\boldsymbol{\omega}$ and $\mathbf{g}$.

When $\gamma \neq \frac{1}{2}\pi$, or when $\gamma = \frac{1}{2}\pi$ and $\lambda > 1$, the dipole axis of the sphere tends in time to a certain fixed orientation which is independent of its initial orientation. The particle then simply rotates about this axis with an angular velocity $\mathbf{e}(\boldsymbol{\omega}.\mathbf{e})$. We refer the reader to the works of Hall & Busenberg (1969) and Brenner (1970*a*, *b*) for a more complete description of this situation.

The special case when $\gamma = \frac{1}{2}\pi$ and $\lambda \leqslant 1$ exhibits a considerably different behaviour. The particle dipole axis does not tend to any fixed orientation, but rather traverses one of an infinite family of periodic closed orbits. In each orbit, the dipole axis describes a circular cone about a fixed central axis of rotation. Brenner (1970*a*) has shown that both the direction of the rotation axis and

magnitude of the cone angle may be related to the value of λ and to a constant which labels the particular orbit. Typical orbits for values of λ near 0, $\frac{1}{2}$ and 1 are sketched in figure 1. The particular closed orbit selected by a particle is determined entirely by its orientation at some initial instant and the given value of λ. Thus, in the absence of rotary Brownian motion (or other non-reversible disturbances), any bulk properties which depend on the orientation distribution of $\mathbf{e}$ would depend for all time on the initial orientation state of the suspension. In this paper we use the basic techniques developed in an earlier investigation (Leal & Hinch 1971, hereafter denoted by LH) to find the orientation distribution which results from the accumulative effects of weak rotary Brownian motions acting over a very long time. As suggested by Brenner & Weissman (1972), the steady-state distribution is independent of the initial orientation state.

In the presence of rotary Brownian motion, the orientation of the dipole axis of any particular particle is determinate only in the statistical sense. We quantify the statistics of the particle orientation by means of the differential probability density function $N(\mathbf{e})$, defined such that the probability of finding a particle with its dipole axis in the solid angle de about $\mathbf{e}$ is simply $N(\mathbf{e})\,de$. Temporal changes in N are governed by a conservation principle

$$\partial N/\partial t + \operatorname{div}\{N\dot{\mathbf{e}} - D\nabla N\} = 0 \tag{2}$$

in which the flux of orientational probability is seen to include advection about the closed orbits and rotary Brownian diffusion. Here $D = kT/8\pi\mu a^3$ is the Stokes–Einstein diffusion coefficient for rotary Brownian motion. The probability density function which is found from (2) is subject to the normalization condition

$$\int N(\mathbf{e})\,de = 1.$$

The particle contribution to the bulk stress in this suspension consists of the familiar Einstein term plus an antisymmetric part due to the net external couple applied to the suspension. Following Brenner & Weissman (1972), we note the expression for the bulk stress

$$\boldsymbol{\sigma} = 2\mu[1+\tfrac{5}{2}\Phi]\,\mathbf{E} - \frac{3m\Phi}{8\pi a^3}[\langle\mathbf{e}\rangle\,\mathbf{g} - \mathbf{g}\langle\mathbf{e}\rangle], \tag{3}$$

in which $\langle\mathbf{e}\rangle$ is the mean of the unit dipole vector,

$$\langle\mathbf{e}\rangle \equiv \int \mathbf{e}N(\mathbf{e})\,de,$$

while Φ is the volume fraction of the spheres and $\mathbf{E}$ is the rate-of-strain tensor for the bulk flow. Hence the calculation of bulk stress for this suspension reduces to finding the mean of the dipole vector.

In the following we consider the case $\gamma = \frac{1}{2}\pi$, $\lambda < 1$, in the limit of weak rotary Brownian motion, $D/\omega \ll (1-\lambda)^{\frac{3}{2}}$. Brenner & Weissman (1972) have studied the nearly isotropic limiting cases $\lambda \ll 1$, $D/\omega = O(1)$; $D/\omega \gg 1$, $\lambda = O(1)$; and $\gamma = \frac{1}{2}\pi$, $D/\omega \ll 1$, $\lambda = O(D/\omega)$, as well as various combinations of γ, λ and D/ω for non-orbiting cases.

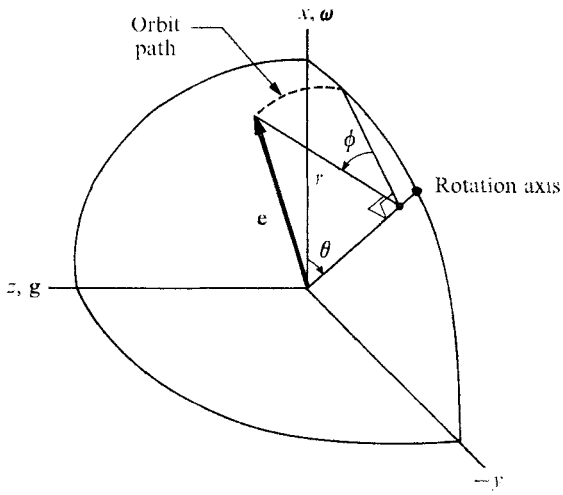

FIGURE 2. Geometry of the orbits; the intrinsic (θ, ϕ) co-ordinate system.

3. Geometry of the closed orbits

For the purposes of the subsequent discussion it is useful to describe the undisturbed particle orbits in greater detail. We use the co-ordinate system shown in figure 2, in which the vorticity and the external field are parallel to the x and z axes, respectively. Following Brenner (1970*a*) we note that the fixed axis of the particle rotation lies in the x, y plane and that the dipole axis sweeps out a circular cone about this axis, with a cone angle which depends on the particular orbit. We specify the orientation of the rotation axis by the polar angle θ as shown in figure 2. In our formulation, θ will play the role of the orbit constant. For a given value of λ, it is easily determined that θ can vary from 0 to $\sin^{-1}\lambda$ while the corresponding cone angle varies from $\frac{1}{2}\pi$ to 0. The orbits of the dipole axis are non-intersecting circles on the unit sphere, which is the domain of the orientation space. Those orbits corresponding to a value of θ in the range $0 \leqslant \sin\theta \leqslant \lambda$ cover the half-sphere above the y, z plane. A set of mirror-image orbits is found in the lower half-sphere. The relative positioning of the orbits changes markedly when λ varies from 0 to 1 as we have indicated in figure 1. When λ is small the maximum permitted θ is similarly small, so that the rotation axes for all the orbits are clustered close to the vorticity axis. The orbits are therefore all circles centred very near to the x axis. On the other hand, as λ approaches 1, the maximum permitted θ tends to $\frac{1}{2}\pi$, so that all the orbits must pass close to the $-y$ axis.

The phase around a particular orbit will be specified by the angle of rotation ϕ measured counterclockwise about the rotation axis, as shown in figure 2. Let the projection of $\mathbf{e}$ onto the rotation axis be $(1-r^2)^{\frac{1}{2}}$, so that the semi-vertex angle of the circular cone swept out by the dipole vector is $\sin^{-1} r$. In these terms, the unit dipole vector may be expressed in component form as

$$\mathbf{e} = \{(1-r^2)^{\frac{1}{2}}\cos\theta + r\cos\phi\sin\theta,\ -(1-r^2)^{\frac{1}{2}}\sin\theta + r\cos\phi\cos\theta,\ r\sin\phi\} \quad (4)$$

and equation (1) describing the axis orbits reduces to

$$r = \text{constant}, \quad \sin\theta = \lambda(1-r^2)^{\frac{1}{2}}, \quad \dot{\phi} = \omega(\cos\theta + r\lambda\cos\phi). \qquad (5a,b,c)$$

Equation (5*b*) provides the necessary relationship between the orbit constant and the cone angle.

Equation (4) is now viewed as the definition of a co-ordinate transformation from (e_x, e_y, e_z) on the unit sphere to the more convenient non-orthogonal co-ordinates (θ, ϕ). Using (5*b*) to eliminate r, the transformation is

$$\lambda e_x = \sin\theta\cos\theta + (\lambda^2 - \sin^2\theta)^{\frac{1}{2}}\sin\theta\cos\phi, \qquad (6a)$$

$$\lambda e_y = -\sin^2\theta + (\lambda^2 - \sin^2\theta)^{\frac{1}{2}}\cos\theta\cos\phi, \qquad (6b)$$

$$\lambda e_z = (\lambda^2 - \sin^2\theta)^{\frac{1}{2}}\sin\phi \qquad (6c)$$

and the orbit equation (1) reduces to

$$\dot{\phi} = \omega[\cos\theta + (\lambda^2 - \sin^2\theta)^{\frac{1}{2}}\cos\phi] \qquad (7)$$

with θ constant. According to (7) the rate of rotation of the dipole axis varies, for a given orbit, from a maximum when $\phi = 0$ to a minimum when $\phi = \pi$; and between the different orbits, from a constant rate $(1-\lambda^2)^{\frac{1}{2}}$ for the trivial orbit ($\sin\theta = \lambda$) to a maximum oscillation $1+\lambda\cos\phi$ for the orbit in the plane perpendicular to the vorticity ($\sin\theta = 0$). Hence there is little variation in $\dot{\phi}$ for small λ, whereas the variation between the orbits and around each orbit becomes very large as λ tends up to unity. In the latter case we note that any particle would spend most of its time nearly aligned with the $-y$ axis, in fact, within a small angle of $O[(1-\lambda)^{\frac{1}{2}}]$ of full alignment.

Equation (7) may be integrated to yield the phase angle ϕ as a function of time:

$$\tan\frac{\phi}{2} = \left\{\frac{\cos\theta + (\lambda^2 - \sin^2\theta)^{\frac{1}{2}}}{\cos\theta - (\lambda^2 - \sin^2\theta)^{\frac{1}{2}}}\right\}^{\frac{1}{2}} \tan\left(\frac{(1-\lambda^2)^{\frac{1}{2}}\,\omega t}{2}\right).$$

As was previously noted, the particle dipole axis describes a periodic orbit. The orbit period $2\pi/(1-\lambda^2)^{\frac{1}{2}}$ is the same for all orbits, with a given value of λ.

We finally turn to the metric of the non-orthogonal θ, ϕ co-ordinates. In addition to the familiar measures of length h_θ and h_ϕ along the curves of constant ϕ and θ respectively, it is necessary to specify the angle α of the skewness between these curves. The three quantities are found from the square of the element of arc length on the unit sphere:

$$ds^2 = h_\theta^2 d\theta^2 + 2h_\theta h_\phi \cos\alpha\, d\theta\, d\phi + h_\phi^2 d\phi^2.$$

Using (6) we find

$$\left.\begin{aligned} h_\theta &= \left[\frac{\lambda^2 - \sin^4\theta}{\lambda^2 - \sin^2\theta} + \frac{2\lambda\cos\theta\cos\phi}{(\lambda^2 - \sin^2\theta)^{\frac{1}{2}}} + (\lambda^2 - \sin^2\theta)\cos^2\phi\right]^{\frac{1}{2}}\lambda^{-1}, \\ h_\phi &= (\lambda^2 - \sin^2\theta)^{\frac{1}{2}}\lambda^{-1}, \\ \tan\alpha &= \frac{\lambda\cot\theta}{(\lambda^2 - \sin^2\theta)^{\frac{1}{2}}\sin\phi} + \frac{\lambda\cot\phi}{\sin\theta}. \end{aligned}\right\} \qquad (8)$$

Hence the important measure of an element of area in the θ, ϕ co-ordinates is

$$h_\theta h_\phi \sin\alpha\, d\theta\, d\phi = [\cos\theta + (\lambda^2 - \sin^2\theta)^{\frac{1}{2}}\cos\phi]\,\lambda^{-1}\,d\theta\, d\phi.$$

4. The orientation distribution function with weak Brownian motion

In this section, we calculate the orientation distribution for the limiting case of weak Brownian motion. The problem is very similar to one discussed in our earlier paper LH, and as we proceed we shall rely heavily on the ideas as presented in that paper. In particular, for this limiting case the calculation of the orientation distribution will be seen to split into two parts: a straightforward determination of the distribution of phase angles for a given orbit, followed by a less obvious calculation of the relative distribution of the different orbits. The effect of the weak Brownian motions over a long time is to damp out the temporal oscillations of the phase distribution and to control the orbit distribution.

We start by transforming (2) into the non-orthogonal θ, ϕ co-ordinates. No large gradients develop in this problem as $D/\omega \to 0$, so that, as we are only interested in the lowest approximation to the distribution function, we omit the Laplacian term. Thence the equation for the steady distribution is simply

$$(h_\theta h_\phi \sin\alpha)^{-1}\,\partial(h_\theta h_\phi \sin\alpha\,\dot{\phi} N)/\partial\phi = 0. \tag{9}$$

This equation expresses the undetered motion of the particles around the orbits in the presence of vanishing Brownian effects. It is solved simply and yields

$$N = \frac{\omega f(\theta)}{h_\theta h_\phi \sin\alpha\,\dot{\phi}} = \frac{\lambda f(\theta)}{[\cos\theta + (\lambda^2 - \sin^2\theta)^{\frac{1}{2}}\cos\phi]^2}. \tag{10}$$

The advantage of the natural θ, ϕ co-ordinate system is that the orientation distribution function resolves itself into two separate components: the denominator of (10) represents the distribution of phase angles about a particular orbit, and the numerator represents the relative distribution between the different orbits.

At the level of approximation represented by (9), the orbit distribution $f(\theta)$ remains undetermined – this reflects the lack of intrinsic preference for any particular orbit which is inherent in (5) when Brownian rotation is completely neglected. The cumulative effect on the orbit distribution of weak Brownian motions over a sufficiently long time is found from a more careful examination of (2). In our earlier paper LH we showed in some detail that the steady orientation distribution satisfies an integral constraint

$$0 = \oint_{\text{orbit}} \frac{\partial N}{\partial n}\,ds = \oint_{\text{orbit}} \left\{\frac{h_\phi}{h_\theta \sin\alpha}\frac{\partial}{\partial\theta} - \cot\alpha\frac{\partial}{\partial\phi}\right\} N\,d\phi.$$

This equation says that in the steady state there is no net diffusion of probability out of each closed orbit. Substituting for N from (10) and performing the indicated integrations yields a first-order ordinary differential equation for $f(\theta)$:

$$[2 + \lambda^2 - 3\sin^2\theta]\,df/d\theta - 6\sin\theta\cos\theta f = 0$$

with solution

$$f(\theta) = \text{constant}/(2 + \lambda^2 - 3\sin^2\theta). \tag{11}$$

The unspecified constant is to be determined from the normalization. This distribution shows a maximum population for the orbit taking the largest permitted value of $\theta(\sin^{-1}\lambda)$ and a minimum for the orbit with $\theta = 0$. The degree of skewness in the orbit distribution becomes more marked as λ approaches unity. The

nearly flat distribution for small λ is expected because the orbits are themselves almost uniformly distributed through the orientation space when labelled by the variable θ. On the other hand, as $\lambda \to 1$, all the orbits crowd through a narrow region near to the y axis. There is consequently a more substantial redistribution towards orbits with larger values of θ in order to reduce the gradient in N near the y axis.

The normalization of f is found from the normalization of N. Considering only the upper half-sphere of the orientation space,

$$\int_0^{\sin^{-1}\lambda} \int_0^{2\pi} N h_\theta h_\phi \sin\alpha \, d\phi \, d\theta = \tfrac{1}{2}$$

or in terms of f

$$\int_0^{\sin^{-1}\lambda} f(\theta) \, d\theta = \frac{(1-\lambda^2)^{\frac{1}{2}}}{4\pi}.$$

The weighting for each orbit is the same because their periods are equal. By performing the integration of (11), we obtain the normalization constant:

$$\text{constant} = (1-\lambda^2)(2+\lambda^2)^{\frac{1}{2}} \left[2\pi \log \frac{(2+\lambda^2)^{\frac{1}{2}}+\lambda}{(2+\lambda^2)^{\frac{1}{2}}-\lambda} \right]^{-1}. \tag{12}$$

Finally, combining (10), (11) and (12) the orientation distribution function may be written as

$$N(\theta,\phi) = \frac{\lambda(1-\lambda^2)(2+\lambda^2)^{\frac{1}{2}}}{2\pi \log \dfrac{(2+\lambda^2)^{\frac{1}{2}}+\lambda}{(2+\lambda^2)^{\frac{1}{2}}-\lambda}} \left[\frac{1}{2+\lambda^2-3\sin^2\theta} \right] \frac{1}{[\cos\theta + (\lambda^2-\sin^2\theta)^{\frac{1}{2}}\cos\phi]^2}. \tag{13}$$

This completes our calculation of the lowest approximation to the distribution function N. Higher approximations could be obtained via a perturbation expansion in the small parameter D/ω as expounded by us in Hinch & Leal (1972). However, for our present purposes it is sufficient to limit considerations to the approximation (13).

5. The particle contribution to the bulk stress

We have given in (3) the expression for the bulk stress and noted that its evaluation in the present circumstances essentially involves a calculation of the mean of the dipolar vector $\mathbf{e}$. Only the component $\langle e_y \rangle$ is significant for calculation of the bulk stress. The component $\langle e_x \rangle$ is identically zero since the y, z plane is a plane of symmetry for the distribution, and the component $\langle e_z \rangle$ is irrelevant since it is parallel to the vector $\mathbf{g}$. Thus, our task reverts to a calculation of $\langle e_y \rangle$:

$$\lambda \langle e_y \rangle = 2 \int_0^{\sin^{-1}\lambda} d\theta \int_0^{2\pi} d\phi \, [-\sin^2\theta + (\lambda^2-\sin^2\theta)^{\frac{1}{2}} \cos\theta \cos\phi] \, N h_\theta h_\phi \sin\alpha.$$

Substituting for N and $h_\theta h_\phi \sin\alpha$ from (10) and (8) and integrating with respect to ϕ we find

$$\lambda \langle e_y \rangle = \left[-1 + 4\pi \int_0^{\sin^{-1}\lambda} \cos\theta f(\theta) \, d\theta \right].$$

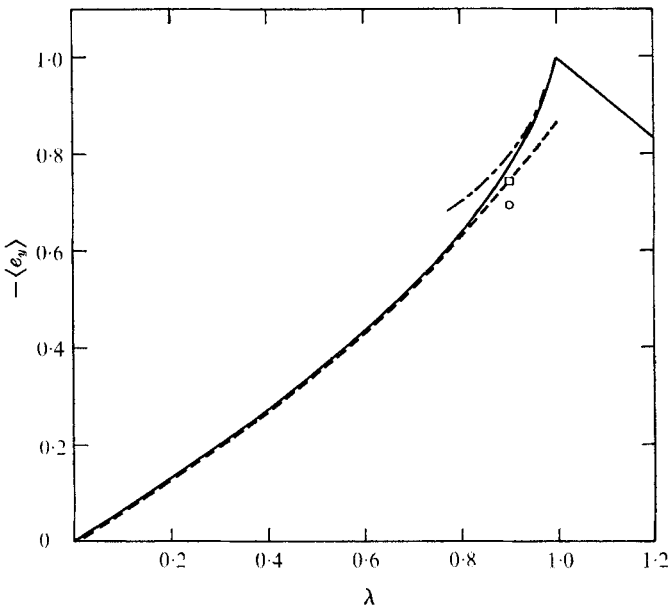

FIGURE 3. The average of the y component of the dipole axis unit vectors. ——, equation (14); – – – –, equation (15); — — —, equation (16). Calculated values from Brenner & Weissman (1972): ○, $\omega/D = 20$; □, $\omega/D = 40$.

Finally, inserting the expression for f from (11) and the normalization constant (12) and performing the θ integration we have

$$\langle e_y \rangle = -\frac{1}{\lambda}\left\{1 - \frac{1-\lambda^2}{3^{\frac{1}{2}}} \frac{\log\{[(2+\lambda^2)^{\frac{1}{2}} + \lambda 3^{\frac{1}{2}}]/[(2+\lambda^2)^{\frac{1}{2}} - \lambda 3^{\frac{1}{2}}]\}}{\log\{[(2+\lambda^2)^{\frac{1}{2}} + \lambda]/[(2+\lambda^2)^{\frac{1}{2}} - \lambda]\}}\right\}. \tag{14}$$

This expression is the main result of our paper.

It is useful to look at the asymptotic evaluation of (14) in the two limits $\lambda \to 0$ and $\lambda \to 1$. Although these asymptotic forms do not match in the commonly accepted sense, between them they do give a remarkably good numerical estimate of (14) throughout the entire range $0 \leqslant \lambda \leqslant 1$. For small λ,

$$\langle e_y \rangle = -\tfrac{2}{3}\lambda - \tfrac{7}{45}\lambda^2 - \tfrac{46}{945}\lambda^3 + O(\lambda^4). \tag{15}$$

The first pair of terms can be found in Brenner & Weissman's (1972) limiting study for $D/\omega \to 0$ with $\lambda = O(D/\omega)$. In the opposite limit, $\lambda \to 1$, we find

$$\langle e_y \rangle = -1 + \epsilon\left[\frac{\log(1/\epsilon) + \log 3}{\frac{1}{2}3^{\frac{1}{2}}\log[(3^{\frac{1}{2}}+1)/(3^{\frac{1}{2}}-1)]} - 1\right] + O\left(\epsilon^2 \log\frac{1}{\epsilon}\right), \tag{16}$$

in which $\epsilon \equiv 1 - \lambda \ll 1$. We have plotted our main result as well as these asymptotic forms in figure 3. We also give two relevant points from Brenner & Weissman's numerical calculations and a portion of the curve $\langle e_y \rangle = -\lambda^{-1}$, which is applicable for weak Brownian motions when $\lambda > 1$. It can be seen that the numerical results for $\omega/D = 20$ and $\omega/D = 40$ are satisfactorily tending to our result (14), which is strictly valid only in the limit $\omega/D \to \infty$.

The results may be understood as follows. When $\lambda \to 0$, we have already noted that all the orbits tend to circle about the vorticity axis with a nearly uniform rate of rotation. So $\langle e_y \rangle$ approaches zero. The slightly negative value is due to the slight skewness of the orbit paths towards negative y and the slightly non-uniform rotation rate, which is slowest as the dipole axis crosses the negative-y axis. At a higher approximation these two effects are partially reduced by the slight drift to orbits with larger values of θ. As λ increases the orbit paths become increasingly skewed towards the negative-y axis, and in the limit as $\lambda \to 1$, they all pass essentially through this point. In addition, especially for small θ, the rate of rotation also becomes skewed and particles eventually spend a very long portion of every orbit with the dipole axis virtually aligned in the direction of negative y. The combination of these two effects then leads to a very large peak in the orientation distribution function near to the negative-y axis. Because of the resulting large gradients in N, rotary Brownian motion acts to produce a net flux away from this position and this leads to a somewhat skewed distribution which favours orbits with $\sin\theta \sim \lambda$. From our result $\langle e_y \rangle \to -1$ as $\lambda \to 1$, it is obvious that the diffusion is not too effective in smoothing N. The reason lies in the nature of the orbits themselves. In diffusing away from the population peak, the particles first encounter orbits of larger θ, but these are themselves nestled relatively near to the y axis. Further outward diffusion puts the particle back onto orbits of small θ. The steady-state distribution then represents a balance between diffusion outwards away from the axis, and advection back, with advection winning because of the assumed smallness of D. The above discussion of the limit $\lambda \to 1$ indicates that our solution is valid only for fixed $\lambda < 1$ as $D/\omega \to 0$. As the gradients become larger and the particle's motion slower within the small region near to the negative-y axis, the diffusion coefficient has to be made progressively smaller in order that the poor advection should win, as we have basically assumed. To correctly estimate the required smallness of the diffusion coefficient we follow our earlier paper LH and ask that the appropriate Péclet number be large, i.e.

$$D/\omega \ll (1-\lambda)^{\frac{3}{2}}.$$

This is the condition quoted without justification earlier in the paper. For a small value of D/ω which does not satisfy this additional restriction, a matched asymptotic expansion must be used which incorporates a singular region near the $-y$ axis (cf. the intermediate regime of Hinch & Leal 1972).

Finally, we consider a simple shear flow

$$\mathbf{u} = (0, 0, \omega y).$$

We chose this particular form for convenience: any simple shear of this magnitude in the y, z plane would do for the present purposes. With this shear flow, the equation for the bulk stress (3) yields

$$\sigma_{yz} = \mu\omega[1 + \tfrac{5}{2}\Phi - \tfrac{3}{2}\Phi\lambda\langle e_y \rangle],$$
$$\sigma_{zy} = \mu\omega[1 + \tfrac{5}{2}\Phi + \tfrac{3}{2}\Phi\lambda\langle e_y \rangle],$$

all other components of the deviatoric bulk stress vanishing. It has become customary to call the tangential shear stress σ_{yz} divided by the shear rate ω

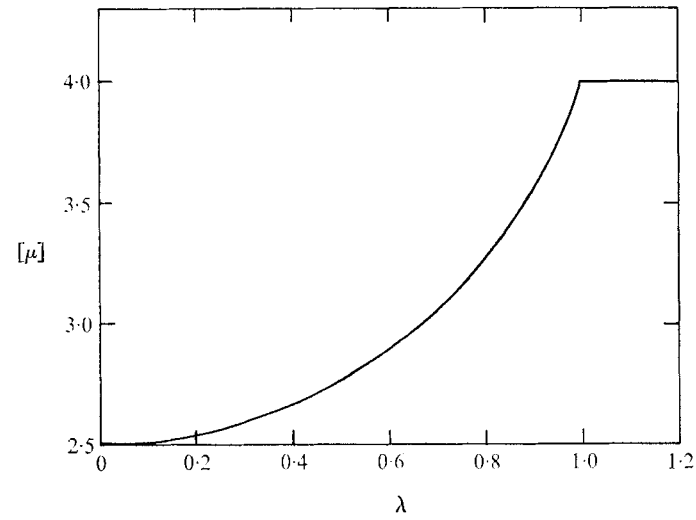

FIGURE 4. The intrinsic viscosity in simple shear flow.

the effective viscosity of the suspension. For a non-Newtonian material this terminology can be misleading; for a discussion of this point in the context of dipolar suspensions see Leal (1971). The intrinsic viscosity is then defined as

$$[\mu] = \lim_{\Phi \to 0} \frac{\sigma_{yz} - \mu\omega}{\mu\omega\Phi}$$

and in the present case is given by

$$[\mu] = \tfrac{5}{2} - \tfrac{3}{2}\lambda\langle e_y \rangle, \tag{17}$$

We have plotted this quantity (for $\lambda \leqslant 1$) in figure 4 with $\langle e_y \rangle$ evaluated from (14). Also plotted is a portion of the weak Brownian motion result for the non-orbiting case

$$[\mu] = 4 \quad (\lambda > 1),$$

which follows from $e_y = -\lambda^{-1}$. It can be seen that the slope of $[\mu]$ versus λ is discontinuous at $\lambda = 1$. For all $\lambda > 1$, the particle dipole axis lies in the y, z plane, the particle does not rotate, and since the disturbance flow caused by the particle is thus independent of λ, the intrinsic viscosity is constant. For $\lambda \leqslant 1$, however, the rotation axis lies in the x, y plane and the particle rotates at a rate depending on the degree of alignment of this axis with the vorticity vector. Since the average degree of alignment increases as λ decreases, the intrinsic viscosity approaches the Einstein value of $\frac{5}{2}$. The discontinuity in the slope of $[\mu]$ is ultimately smoothed out in a small region $\lambda = 1 + O(D/\omega)^{\frac{2}{3}}$, which could be examined using the matched asymptotic expansion mentioned earlier.

It is interesting to compare our results with those for the weak Brownian motion for $\gamma \neq \frac{1}{2}\pi$. Brenner (1970*b*) has given the intrinsic viscosity for the limiting case $D/\omega = 0$ as

$$\tfrac{5}{2} + \tfrac{3}{4}\{1 + \lambda^2 - [(1-\lambda^2)^2 + 4\lambda^2\cos^2\gamma]^{\frac{1}{2}}\}.$$

This takes a well-defined limit for fixed λ as $\gamma \to \frac{1}{2}$, which is

$$\begin{aligned} &\tfrac{5}{2}+\tfrac{3}{2}\lambda^2 \quad \text{for} \quad \lambda < 1, \\ &4 \qquad\qquad\ \ \text{for} \quad \lambda > 1. \end{aligned}$$

It is clear that this limiting result for $\gamma \to \frac{1}{2}\pi$ differs from our results for weak Brownian motion at $\gamma = \frac{1}{2}\pi$. The apparent disagreement is resolved by carefully considering the double limit, $D/\omega \to 0$ and $\gamma \to \frac{1}{2}\pi$. For γ near but not equal to $\frac{1}{2}\pi$, the particle tends to its fixed orientation via a spiral path which differs little from the closed orbits for $\gamma = \frac{1}{2}\pi$. It is useful to describe the spiralling as a combination of motion about the orbits with a cross-orbit drift. When Brownian rotation is negligible, the cross-orbit drift eventually yields the preferred particle orientation and Brenner's limiting expression for $[\mu]$ is valid. On the other hand, when γ is very near to $\frac{1}{2}\pi$, the cross-orbit drift is very slow and is easily dominated by Brownian rotations, so that the particle effectively follows the closed orbits for $\gamma = \frac{1}{2}\pi$. In those circumstances, our present analysis would be applicable. An estimate of the magnitude of D/ω separating these two regimes is obtained by noting that the rate of convergence of the spiral 'orbit' to its fixed point is of $O(\omega\lambda|\gamma-\frac{1}{2}\pi||1-\lambda|^{-\frac{1}{2}})$ so long as $|\gamma-\frac{1}{2}\pi| \leqslant |1-\lambda|$ and $\lambda = O(1)$. Thus for fixed λ, as $\gamma \to \frac{1}{2}\pi$, the particle will ultimately attain an equilibrium orientation provided that

$$D/\omega \ll |\gamma-\tfrac{1}{2}\pi||1-\lambda|^{-\frac{1}{2}}, 1.$$

As γ becomes sufficiently close to $\frac{1}{2}\pi$ for this restriction to be violated, then our regime takes over, and the expression (17), with (14), becomes valid for the intrinsic viscosity. Thus for any fixed $\gamma \neq \frac{1}{2}\pi$, there exists a D/ω sufficiently small for Brenner's regime to be applicable. However, as $\gamma \to \frac{1}{2}\pi$ for D/ω fixed and small, there will always be a smooth transition from Brenner's regime to the regime of our present analysis.

During this work EJH was supported by the California Institute of Technology as a visitor in Applied Mathematics. Acknowledgement is made to the donors of the Petroleum Research Fund, administered by the American Chemical Society, for partial support of LGL.

REFERENCES

Brenner, H. 1970*a* *Annual Rev. Fluid Mech.* **2**, 137.
Brenner, H. 1970*b* *J. Colloid & Interface Sci.* **32**, 141.
Brenner, H. & Weissman, M. H. 1972 *J. Colloid. & Interface. Sci.* to appear.
Hall, W. F. & Busenberg, S. N. 1962 *J. Chem. Phys.* **51**, 137.
Hinch, E. J. & Leal, L. G. 1972 *J. Fluid Mech.* **52**, 683.
Leal, L. G. 1971 *J. Fluid Mech.* **46**, 395.
Leal, L. G. & Hinch, E. J. 1971 *J. Fluid Mech.* **46**, 685.